J Neurophysiol 98: 3109–3118, 2007.
First published September 12, 2007; doi:10.1152/jn.00569.2007.

Compact Movable Microwire Array for Long-Term Chronic Unit Recording in Cerebral Cortex of Primates

Andrew Jackson[1] and Eberhard E. Fetz[2]

[1]*School of Neurology, Neurobiology and Psychiatry, University of Newcastle, Newcastle-upon-Tyne, United Kingdom; and* [2]*Department of Physiology and Biophysics and Washington National Primate Research Center, University of Washington, Seattle, Washington*

Submitted 22 May 2007; accepted in final form 10 September 2007

Jackson A, Fetz EE. Compact movable microwire array for long-term chronic unit recording in cerebral cortex of primates. *J Neurophysiol* 98: 3109–3118, 2007. First published September 12, 2007; doi:10.1152/jn.00569.2007. We describe a small, chronically implantable microwire array for obtaining long-term unit recordings from the cortex of unrestrained nonhuman primates. After implantation, the depth of microwires can be individually adjusted to maintain large-amplitude action potential recordings from single neurons over many months. We present data recorded from the primary motor cortex of two monkeys by autonomous on-board electronic circuitry. Waveforms of individual neurons remained stable for recording periods of several weeks during unrestrained behavior. Signal-to-noise ratios, waveform stability, and rates of cell loss indicate that this method may be particularly suited to experiments investigating the neural correlates of processes extending over multiple days, such as learning and plasticity.

INTRODUCTION

Extracellular recordings of action potentials ("spikes") in awake, behaving primates provide unique insights into the neural control of complex behavior. Conventionally, a recording chamber is positioned over a craniotomy and sharp microelectrodes are lowered through the dura into the cerebral cortex of restrained animals performing trained tasks (Lemon 1984). Commercially available electrode drives, including those from Thomas Recording (Baker et al. 1999; Eckhorn and Thomas 1993), Alpha-Omega Engineering (Johnson and Welsh 2003), and Nan Instruments, allow multiple microelectrodes to be independently positioned on a daily basis, although head fixation is usually required to stabilize recordings and the range of movement tasks that can be studied with this paradigm is limited. Furthermore, electrodes must be removed at the end of each recording session, making this method unsuitable for investigating neural correlates of processes that take several days or more, such as cortical plasticity during skill learning. Recently, chronically implanted electrodes have been developed to follow cells long term without the need for head fixation or restraint. Common electrode designs include thin, flexible microwires (Kralik et al. 2001) or micromachined silicon probes (Nordhausen et al. 1996; Suner et al. 2005) and, in the future, such devices may have clinical application in a new generation of neural prostheses and brain–computer interfaces (BCIs) controlled by real-time spike recordings (Nicolelis 2003; Schwartz et al. 2006). However, a common disadvantage of current techniques is the need to permanently fix electrodes in place at the time of surgery. Gauging the correct depth may be difficult if spontaneous firing rates under anesthesia are low and there is no possibility of subsequently moving electrodes to sample new cells or record from deeper tissue, such as in the banks of sulci. Furthermore, gliosis and cell death around implanted electrode tips cause a reduction in recording quality over time (Biran et al. 2005; Griffith and Humphrey 2006; Szarowski et al. 2003). A movable design could extend the usable lifetime of these implants and provide more comprehensive sampling of neural responses from a cortical area by allowing electrodes to be repositioned as needed in fresh tissue.

In small mammals, miniature microdrives attached to the skull have been successfully used to study neural activity during unrestrained behavior (Kralik et al. 2001; O'Keefe and Recce 1993; Swadlow et al. 2005; Wilson and McNaughton 1993). However, their application in primates is limited by the tougher dura mater and large subarachnoid space within which the brain moves in relation to the skull. Even a slight movement of the brain will cause substantial changes in the size of action potentials recorded by sharp electrodes penetrating the dura. Larger movements may result in tissue injury. Although such techniques can initially provide a good yield of cells after moving electrodes into fresh tissue, the long-term stability of cortical recordings seems limited to a few days at most (Gray et al. 2006; Wilson et al. 2003).

We are developing low-power, implantable electronic devices that monitor and modulate neural activity in freely behaving primates to explore long-term plasticity induced by recurrent BCIs (Jackson et al. 2006a,b; Mavoori et al. 2005). To obtain stable recordings of the same isolated single units over many days and to sample new cells with good signal-to-noise characteristics over long experimental periods we have developed a technique to implant movable microwire arrays in the cortex of primates. The arrays are easily constructed from readily available materials and yield high-quality, stable recordings of the same single units for $\geq$1 wk at a time. By periodically moving the wires we have been able to obtain large spike waveforms and clean recordings over experimental periods of $>$1 yr from the same area of cortex. Herein we describe the construction of the implant and document the recording quality and stability of spike waveforms obtained from implants in the hand area of primary motor cortex (M1) of two monkeys. Some of these data were collected as part of previously reported experiments (Jackson et al. 2006a, 2007).

Address for reprint requests and other correspondence: A. Jackson, Sir James Spence Institute, Royal Victoria Infirmary, Queen Victoria Road, Newcastle-upon-Tyne NE1 4LP, UK (E-mail: andrew.jackson@ncl.ac.uk).

The costs of publication of this article were defrayed in part by the payment of page charges. The article must therefore be hereby marked "*advertisement*" in accordance with 18 U.S.C. Section 1734 solely to indicate this fact.

METHODS

Implant design

The microwire implant consisted of 12 Teflon-insulated 50-μm-diameter tungsten wires running inside polyamide guide tubes. The wires entered the brain through an opening in the dura within a small craniotomy that was subsequently closed with dental cement. The guide tubes themselves were filled with antibiotic ointment and sealed at both ends with Silastic. This waterproof seal prevented infection tracking into the brain and allowed experiments to be performed over many months with minimal chamber maintenance. The microwires slid freely through the Silastic seal, allowing the depth of each to be individually adjusted at any stage by grasping the wire above the guide tube with forceps. The entire assembly was housed within a lidded titanium casing attached with screws to the skull. For these experiments a 6-cm-diameter cylindrical casing contained a single microwire array in M1, as well as our Neurochip electronics and battery.

Implant construction

The microwire implant consisted of two components constructed separately: an array of guide tubes to align the microwires and a connector block for making electrical contacts. Figure 1 shows the assembly procedure. The guide tubes were made from 40-mm lengths of polyamide tubes with 225-μm internal diameter (part #822200, A-M Systems, Carlsborg, WA), threaded onto tungsten rods and aligned in the desired spatial arrangement. This was performed by taping the ends of the rods to a piece of card with a cut-out window (Fig. 1*A*). Two rows of six rods were taped to each side of the card to produce a 6 $\times$ 2 array. Once all the tubes lay parallel they were fixed at one end with a small amount of dental cement. After this had hardened, the rods at the other end were splayed and more dental cement was applied. The result was a fan-shaped arrangement of tubes with a spacing of about 2 mm along one side and 300 μm along the other (Fig. 1*B*).

Centiloc-series pin connectors (part #031-9540-000; ITT Cannon, Santa Ana, CA) were crimped to 15-cm lengths of tungsten microwire (part #795500, A-M Systems) and slotted through holes in a 4 $\times$ 3-way plastic connector block (part #CTA4-IP-60, ITT Cannon). The connector was held upside-down with the wires aligned in parallel down one side by threading them through holes in a spacer and weighting each with an alligator clip (Fig. 1*C*). Slow-setting epoxy was applied to the base and side of the connector to insulate the contacts and fix the wires. The connector was then rotated by 90° so the bent wires projected from the side of the connector, where a one-part Silastic (type A; Dow Corning, Midland, MI) was applied to add strain relief (Fig. 1, *D* and *E*).

At this stage, both components were sterilized by overnight (minimum 10 h) immersion in freshly activated glutaraldehyde sterilization fluid (Cidex Plus, Johnson & Johnson Medical Products); the tungsten rods were removed while the array was submerged to draw fluid into the interiors of the guide tubes. The final assembly process was completed under aseptic conditions with sterile tools. After flushing with sterile water, each guide tube was filled with antibiotic cream (Gentak; Akorn, Buffalo Grove, IL) by injection through a 26-gauge needle placed around it. The tubes were then trimmed to a final length of around 20 mm and attached to the connector block with dental cement. The wires were threaded into the guide tubes with the aid of magnifying loupes, and a quick-setting two-part Silastic (Kwik-Sil; WPI, Sarasota, FL) was applied to seal each end. Finally, the microwires were cut to the appropriate length with sharp scissors perpendicular to the long axis, yielding a tip impedance of around 0.5 MΩ at 1 kHz, and retracted so that they protruded only slightly from the Silastic. The assembled implant is shown in Fig. 1*E*.

Implant surgeries

All procedures were approved by the University of Washington Institutional Animal Care and Use Committee. Arrays were implanted in two male *Macacca nemestrina* monkeys (monkey Y: 3 yr, weight: 4.3 kg; monkey K: 3 yr, weight: 4.6 kg). Each animal received corticosteroids [dexamethasone, 1 mg/kg, administered orally (po)] on the night before and at the beginning and end of surgery to reduce cerebral edema. Implantation was performed under aseptic conditions with inhalational anesthetic (isoflurane 2–2.5% in 50:50 O_2:N_2O). Heart rate, blood pressure, temperature, end-tidal CO_2, and blood oxygen saturation were continuously monitored to ensure stable anesthesia, and fluids were administered by an intravenous (iv) catheter. With the animal in a stereotaxic frame, the skin and periosteum over the skull were resected and a craniotomy approximately 10 mm wide was drilled with a dental bur at stereotaxic coordinates A 13 mm and L 18 mm. A skull screw was placed close to the craniotomy to anchor the microwire connector block. Before opening the dura mater, the monkey was hyperventilated slightly to reduce the intracranial pressure. The dura mater was then resected to the edge of the craniotomy, permitting visualization of the central sulcus (CS). Stimuli were delivered through a silver ball electrode placed anterior to the CS to locate the area from which movements of the hand could be elicited with the lowest threshold. To reduce relative movement of the brain and skull and stabilize recordings, the pia mater was bonded to the edge of the craniotomy with cyano-acrylate glue following the method described by Kralik et al. (2001). The microwire array was then lowered into position on a stereotaxic carrier such that the ends of the guide tubes rested just above the pial surface over the hand representation and oriented such that extruded wires would travel along the bank of the precentral cortex. The connector block was securely anchored to the skull screw with dental cement (Fig. 1*F*) and each wire was individually inserted into the cortex by grasping the exposed loop with fine, angled forceps and advancing slowly at a speed of about 1 mm/s. Where possible, penetration of the pia mater was verified through a microscope. We did not record from the wires at the time of surgery, preferring to position them slightly below the surface and advance them further at a later stage under ketamine anesthesia when M1 firing rates are robust. With the dura removed and the guide tubes positioned just above the pial surface, the individually inserted wires easily penetrated the brain without the problems of electrode buckling or tissue dimpling reported with other methods (Kralik et al. 2001; Swadlow et al. 2005). However, it is important to ensure that each wire has penetrated the pia at the time of surgery because the formation of scar tissue may prevent insertion at a later stage. Once all microwires had been inserted, the craniotomy was tightly filled with gelfoam and sealed using dental cement. Care was taken to apply the cement initially in small quantities to avoid heating the tissue. A cross section of the implanted microwire array is shown in Fig. 1*G*.

The titanium casing was attached with further skull screws and cement. To seal the inside of the casing, exposed skull was covered first with a layer of varnish (Copaliner; Bosworth, East Providence, RI) and then with a thin layer of dental cement. The layer of varnish proved useful in preventing fluid leaking from the skull into the casing, which could occur when only dental cement was used. Finally, the skin was drawn around the implant with several sutures. The entire procedure took approximately 5 h and was followed by a full program of analgesics [buprenorphine 0.15 mg/kg, administered intramuscularly (im), and ketoprofen 5 mg/kg, po] and antibiotics (cephalexin 25 mg/kg, po).

Implant maintenance

Every 1–2 wk the monkeys were lightly sedated with ketamine (10 mg/kg, im) to sterilize the inside of the head casing using warmed, dilute chlorohexadine solution followed by isopropol alcohol. If

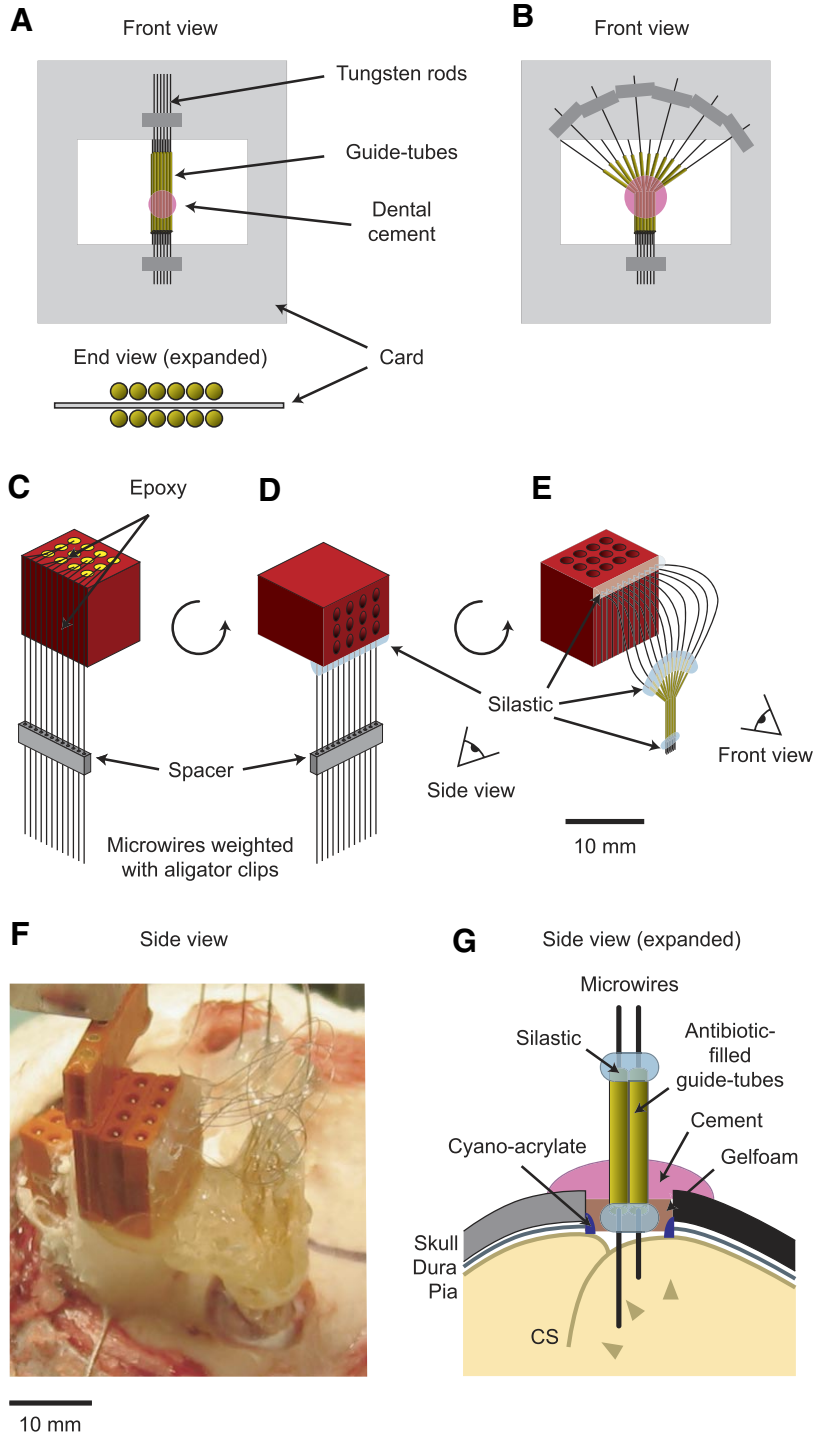

FIG. 1. Construction of the movable microwire array. *A*: guide tubes were first aligned on parallel tungsten rods and fixed with dental cement. Two rows of 6 tubes were positioned on each side of a piece of card to produce a 6×2 array (see expanded end view). *B*: guide tubes were splayed at one end and more cement was applied. *C*: weighted microwires hung parallel along one side of the connector. Epoxy was applied to electrically insulate the contacts and fix the wires. *D*: connector block was rotated and Silastic was applied to the wires for strain relief. *E*: finished implant. Wires ran in loops from the connector block to the guide-tube array. Guide tubes were filled with antibiotic ointment and sealed at both ends with Silastic. *F*: implant as it was fixed to the skull during surgery. Microwires can be seen entering the brain through a craniotomy. *G*: cross section showing microwires penetrating the pia mater anterior to the central sulcus (CS) through a craniotomy and dural opening. Pia mater was bonded to the edge of the craniotomy with cyano-acrylate glue and the craniotomy was sealed with gelfoam and dental cement.

recording quality had deteriorated, or the current sample of cells had been sufficiently characterized for experimental purposes, we took this opportunity to move some or all of the microwires to find new cells. We typically moved between four and eight wires during one of these sessions, aiming to achieve a sample of two to five cells. Our experiments required monitoring individual cells for several days each, so this sample was sufficient for $\geq$1 wk of data collection. Once an appropriate sample of cells was obtained, we avoided moving additional wires to minimize disturbance to the tissue.

While listening to an audio monitor of the recorded signal, the wires were nudged up or down with fine, angled forceps. Care was taken to avoid bending the wires while pushing them down because kinks could prevent free movement through the guide tubes. By grasping the wires only a short distance (no more than a few millimeters) above the top of the guide tube, buckling or kinking of the wires and large, uncontrolled movements could be avoided. Although there is potential for the forceps to damage the insulation around the wires, in our design any breaks at the level that the wires are grasped will remain above or within the sealed guide tubes, preventing any shunting of the recorded signal through the tissue. Often the first movement of a wire after it had remained in place for days or weeks produced large changes in the audio quality, possibly as the tips broke through glial encapsulation. Subsequent movements did not produce such abrupt changes, although an increase in background noise often preceded the

appearance of clean neurons. Unlike isoflurane anesthesia, ketamine sedation is associated with considerable activity in M1. Many neurons fire bursts of action potentials ≤50 Hz followed by periods of quiescence with an overall rhythmicity of around 0.2–0.4 Hz (Steriade et al. 1993), making it possible to position the wires at suitable depths to record units.

Recording

The recordings documented here were obtained with our Neurochip technology, previously described in detail (Jackson et al. 2007; Mavoori et al. 2005). Briefly, this battery-powered electronic implant amplifies, filters, and samples the signal from a single microwire. For these recordings, the gain was set in the range ×1,500–12,000, the filter pass band was 500 Hz to 5 kHz, and the sampling frequency was 11.7 kHz. The Neurochip recorded the raw signal, the rate of spike events accepted by its on-line dual time–amplitude window discriminator algorithm, or some combination of both. Most of the analysis reported here is derived from sequential sections of raw data (~10 min per channel) recorded during the daytime while the monkeys performed a trained wrist-movement task. Overnight records of the firing rate of a single cell were compiled with 100-ms bins and interspersed with 22-ms sections of raw signal every 3 min to assess cell stability. Changes in spike size during overnight recordings were verified in the subsequent daytime session using a fresh battery and a different Neurochip board to ensure these did not arise from nonstationarities in the electronics. During periods of trained behavior, precise times of discriminated spike events were transmitted in real time by infrared to a remote PC. Interspike interval (ISI) histograms compiled from these records were used to distinguish single-unit and multiunit activity. Because transmission of data in this way requires an unbroken line of sight to the implant, we were unable to compile ISI histograms for overnight recordings during unrestrained behavior.

Postmortem histology

At the end of the recording period in monkey Y, a surgical level of anesthesia was induced with sodium pentobarbitone (25 mg/kg, iv) before perfusion through the heart with neutral-buffered formalin. Coronal sections (50 μm) of cortex were stained with cresyl violet. Monkey K is still alive at the time of writing.

Analysis

Off-line, spike events were extracted from the daily raw recordings using the same discrimination algorithm as was implemented in real time by the Neurochip, consisting of a threshold and two time–amplitude windows (Mavoori et al. 2005). Discriminator parameters were adjusted for each day's record to compensate for changes in spike waveform. In general we have found that the recording quality using our Neurochip system is excellent; the short leads to the Neurochip circuit do not pick up interference or generate movement artifacts, and the battery power supply and titanium shielding effectively isolate the recording from other sources of electrical noise and artifacts. Therefore waveforms with peak-to-peak amplitudes ≳100 μV could usually be isolated on the basis of threshold crossing alone, although the subsequent time–amplitude windows were useful for rejecting the occasional erroneous trigger or, in rare cases, separating multiple cells present on the same electrode. We separated multiple cells only when the waveforms were clearly distinct (i.e., the respective time–amplitude windows did not overlap) because overly restrictive discrimination criteria could artificially inflate signal-to-noise measures by rejecting spikes that did not fit a precise template.

Cell identities were verified across multiple days of recording using several factors. We looked for stability of cell waveforms and behavioral tuning assessed both during a trained wrist-movement task and unrestrained behavior (Jackson et al. 2007). Continued identity of those cells for which overnight Neurochip recordings revealed gradual changes in waveforms was accepted so long as ISI histograms indicated that there was only one cell in the recording. If spike waveforms changed abruptly, or when a large change in waveform and/or behavioral tuning occurred on channels that were not tracked using the Neurochip, the cell was considered to have been lost.

Accepted waveforms consisted of sections from 5 sampling points before to 15 sampling points after the threshold crossing (1.7 ms total). Cell size was quantified by averaging peak-to-peak amplitudes across accepted waveforms. In addition, for comparison with a previous report we calculated signal-to-noise ratio (SNR) using the technique described by Suner et al. (2005). In this method, accepted spike waveforms are aligned at the threshold crossing and the peak-to-peak amplitude (A) of the average waveform is calculated. Noise (ε) is quantified by the SD of the residuals remaining after this average is subtracted from each individual waveform, and SNR is calculated as A/ε. Because this calculation relies on precise alignment of the individual waveforms to the threshold crossing, we performed the analysis on data that had been up-sampled by a factor of 4 using low-pass interpolation (MatLab *interp* function) to give an effective sampling resolution of 47 ksp/s. Use of other interpolation methods did not affect the results.

Finally, to evaluate the similarity of different spike shapes we calculated linear correlation (r) values between time-shifted average waveforms (i.e., the cross-correlation function calculated between mean-subtracted, variance-normalized spike shapes). The maximum r value across time shifts was used to quantify similarity, with a value of 1 indicating identical spike shapes irrespective of absolute amplitude differences. Similarity scores were calculated between all waveforms for the same cell recorded on different days and between all pairs of different cells recorded during the experiment.

RESULTS

Data set

This analysis is based on 113 cells (monkey Y: 58 cells; monkey K: 55 cells), of which 88% were verified as clean single units from refractory periods in ISI histograms. This probably represents an underestimate of the maximum cell count that could have been obtained because the single Neurochip recording channel and other experimental considerations meant we could not record from every microwire during every session. However, on the first day after the wires were moved we sampled all channels showing good activity; subsequently we typically followed all these cells on a daily basis during performance of the task while recording individual cells overnight with the Neurochip. Therefore these totals are a realistic estimate of the yield of usable neurons that can be expected in practice under similar experimental conditions.

Spike amplitudes and signal-to-noise ratio (SNR)

Figure 2*A* shows a 1-s section of signal recorded from a microwire that had just been repositioned in M1 (subsequently referred to as day 0). This recording from monkey K was made 77 days after the initial microwire implant surgery. The burst of action potentials was typical of the robust activity seen under ketamine anesthesia and the peak-to-peak amplitude (300 μV) is representative of well-isolated neurons obtained with this implant. Recordings on subsequent days with the monkey awake (Fig. 2*B*, days 1–5) show that the spike shape remained generally stable. On day 6 this large waveform was absent and, although smaller spikes were present in the recording, these had a different modulation with trained wrist move-

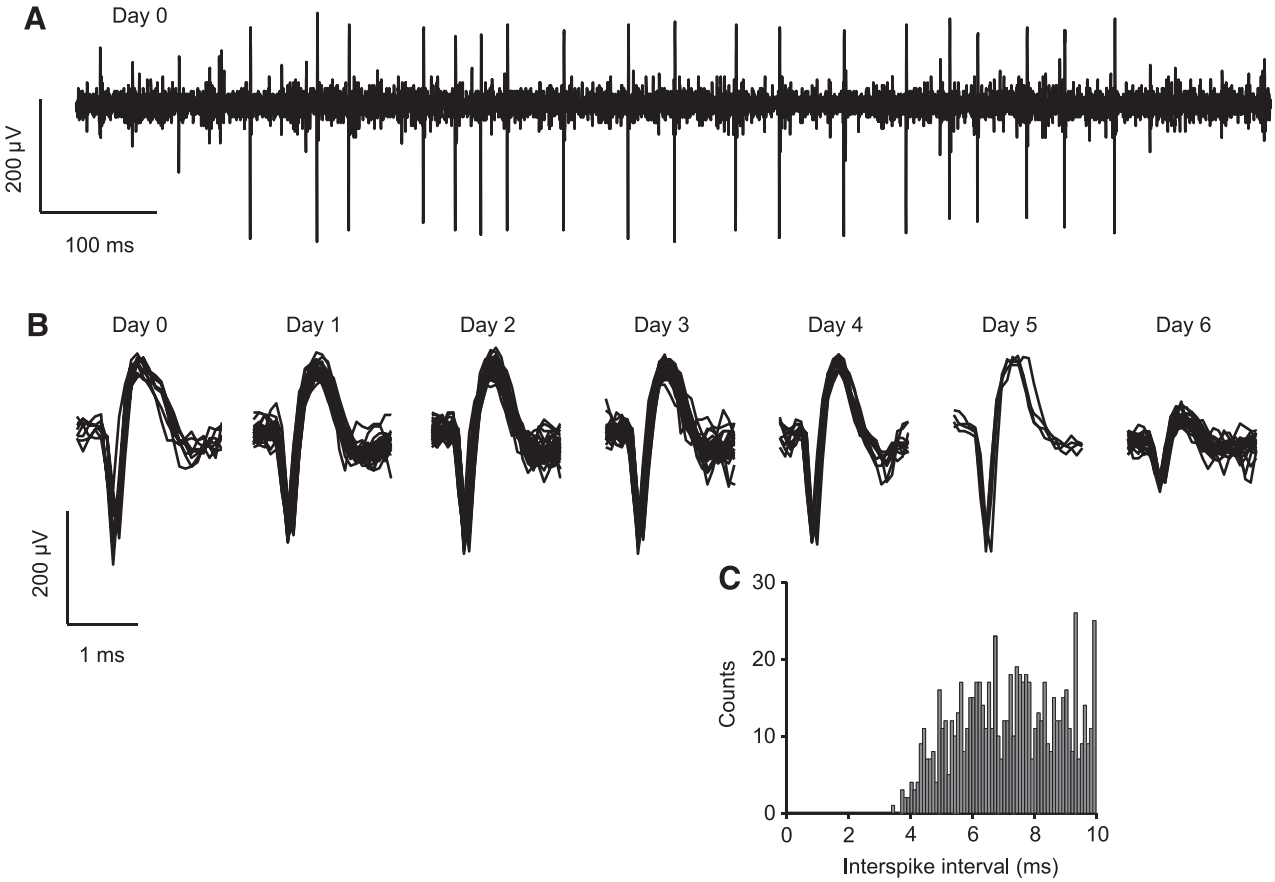

FIG. 2. Sample neuronal recordings from primary motor cortex (M1). *A*: 1-s recording obtained immediately after repositioning a microwire under ketamine sedation (day 0). Subsequent days are indexed relative to this, which corresponds to day 77 after implantation of the array. *B*: superimposed spike waveforms for recordings obtained on day 0 and six subsequent days while the monkey was awake. Larger waveform disappeared abruptly toward the end of day 5. *C*: interspike interval (ISI) histogram compiled for spikes recorded during trained behavior on day 5.

ments, suggesting they arose from a new neuron. The large waveform disappeared abruptly (toward the end of day 5), so it seems likely that movement of the electrode caused the original cell to be lost or injured. The ISI histogram in Fig. 2*C* was compiled from data recorded while the monkey made repeated trained wrist movements on day 5. The absence of short intervals confirms that these waveforms were produced by a single cell (similar results were also obtained for the earlier days).

Figure 3, *A* and *B* plots the peak-to-peak amplitude of all cells recorded in the two animals. Tick marks above each graph indicate occasions when some of the microwires were repositioned under sedation. Combining data across both animals, wires were moved on 39 occasions to yield 113 units at an average of 2.9 cells on each occasion (range 1–9). In monkey Y, despite one cell with an unusually large waveform recorded in early sessions, there was no significant relationship between spike amplitude and the number of days following array implantation (Pearson's $r = -0.25$, two-tail, $P = 0.06$). During the final weeks of the 184-day experimental period, we were still able to record clean units with amplitudes up to 380 μV. In monkey K the amplitudes showed no significant change over a 326-day period ($r = 0.06$, $P = 0.6$). As expected, the amplitudes for waveforms that were classed as multiunit (dark gray, mean 125 μV, SD 32 μV) tended to be smaller than those for single units (light gray, mean 248 μV, SD 158 μV), although a few recordings with spike amplitudes $\leq$180 μV failed to yield cleanly discriminated single units. Figure 3*C* shows a histogram of SNR values for all cells classified as single unit or multiunit. Most multiunit recordings had low SNR values, although one ISI histogram indicated multiple cells despite discriminated waveforms with SNR of almost 17. In this case, the recording probably included two cells with large but similar spike waveforms. Such occurrences underline the importance of compiling ISI histograms to verify clean discrimination rather than relying on SNR alone. SNR values for clean units were generally high (mean 14.5, SD 6.2) and across the population were positively correlated with peak-to-peak amplitudes (Fig. 3*D*, $r = 0.68$, $P < 1e\text{-}6$).

Stability of recordings

Clean single units could often be followed up to several weeks after positioning the microwires. Figure 4*A* shows sample waveforms from one of the most stable cells, which was followed for a period of 17 days. Using the on-board Neurochip electronics, we were able to continuously monitor the firing rate of this cell as the monkey moved freely around the home cage. Interspersed sections of raw recording were used to assess the stability of spike waveforms. Figure 4*B* shows a 20-h record of firing rate covering the period from 16 to 17 days after this microwire had been moved. Mean firing rate decreased during the night, but this drop was not associ-

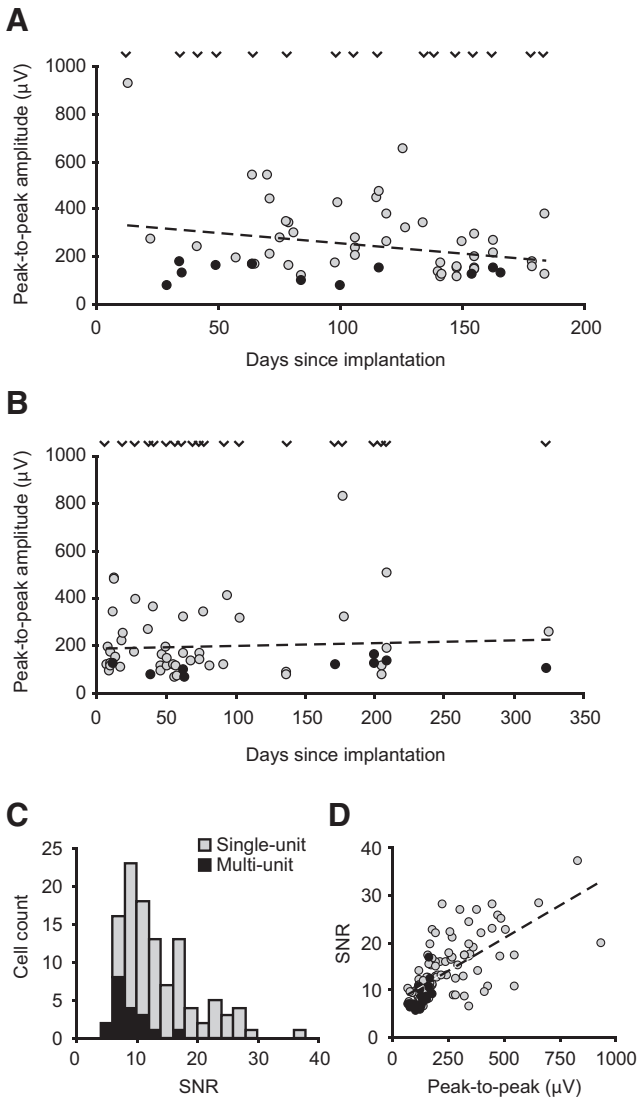

FIG. 3. Long-term performance of movable microwire array. *A*: peak-to-peak amplitude of all single units (light gray circles) and multiunits (dark gray circles) recorded over the lifetime of the implant in monkey Y. Each point represents the amplitude of the cell on the first day that it was recorded. Tick marks above the plot indicate occasions when the microwires were repositioned. Trend line is based on least-squares fitting through all single- and multiunit amplitudes. *B*: comparable plot for monkey K. *C*: histogram of signal-to-noise ratio (SNR) values for single-unit (light gray) and multiunit (dark gray) waveforms. *D*: scatterplot of SNR vs. peak-to-peak amplitude for all cells.

ated with a change in action potential and rates returned to original levels the next morning. ISI histograms compiled from spike events transmitted in real time during trained behavior, combined with the stability of directional tuning (Jackson et al. 2007), strongly suggest that we were recording the same single unit throughout this period. The size and shape of the action potential waveforms remained consistent despite the energetic behavior of the monkeys in the home cage, which included frequent jumping, somersaulting, swinging upside down, and sudden movements of the head.

Although the majority of data sets tracked stable activity, in some cases cells were lost during recording with the Neurochip. Figure 4*C* shows firing rate data collected for one cell between 7 and 8 days after moving this microwire. The recorded rate of spike events classified by the Neurochip declined steadily from 2 a.m. onward. At this point, the monkey was probably asleep, given the periodic fluctuations in firing rate characteristic of sleep cycles (Jackson et al. 2007). Interspersed raw recordings revealed that the decline in detected spike events was caused by a steady reduction in waveform amplitude, such that by 6 a.m. very few spikes satisfied the criteria for discrimination. The amplitude of this cell continued to decline and by day 9 could not be distinguished above the background noise. This suggests that a slow drift or change at the electrode–tissue interface caused steady signal degradation over several days. A different type of unstable recording is shown in Fig. 4*D*. At around 5:30 p.m. on day 4 the rate of discriminated events on this channel fell abruptly to zero. Although small waveforms could subsequently be seen in the recording, it is not possible to know whether any arose from the same cell. Of 26 neurons lost while the Neurochip was recording, the majority (20) declined steadily in amplitude. The remaining 6 disappeared abruptly and all these cases of sudden loss occurred during the daytime. This suggests that abrupt disappearances may be related to movements of the animal, consistent with a previous report (Santhanam et al. 2007). On one occasion the abrupt loss of a cell coincided with observation of the monkey vigorously shaking his head.

For 69 cells that were followed over consecutive recording sessions we calculated the percentage lost per day (Fig. 5*A*). The highest rate of loss (23% or 7/31 cells) occurred immediately after the wires were moved (i.e., between day 0 and day 1). This rate fell to 7% (4/53 cells) between day 1 and day 2, before rising to between 15 and 20% per day over the next few weeks. By cumulatively combining the loss rates from day 1 onward, we predicted the proportion of day 1 cells that would be retained on each subsequent day. This prediction, shown as a dashed line in Fig. 5*B*, suggests that approximately half of the original population of day 1 neurons would be retained after 1 wk and only one tenth after 2 wk. Figure 5*B* also shows the actual proportion of cells that were recorded on each subsequent day (solid line), which falls slightly below the predicted retention rate because we did not always follow every cell until it was lost. Microwires were sometimes moved to sample new cells even if previously documented neurons were still present. Those cells that were not followed over consecutive recording sessions were not included in the calculation of the loss rates (Fig. 5*A*) used to predict the dashed line in Fig. 5*B*.

The average percentage change in peak-to-peak amplitudes of retained cells over successive recordings is shown as solid circles in Fig. 5*C*. On average this was not significantly different from zero over any period tested, suggesting that declining spike amplitudes for some cells were balanced by increases in the amplitude of other cells, particularly between day 0 and day 1. The open circles in Fig. 5*C* plot the average absolute change (i.e., disregarding sign), which decreased steadily over each day after repositioning of the microwires ($r = -0.67$, $P = 0.002$). This may be in part because some unstable cells were lost progressively from the sample, although even those cells that were retained tended to show the largest amplitude changes during the first few days after the wires were moved.

To characterize the similarity between spike shapes recorded from the same cell on different days we calculated the maxi-

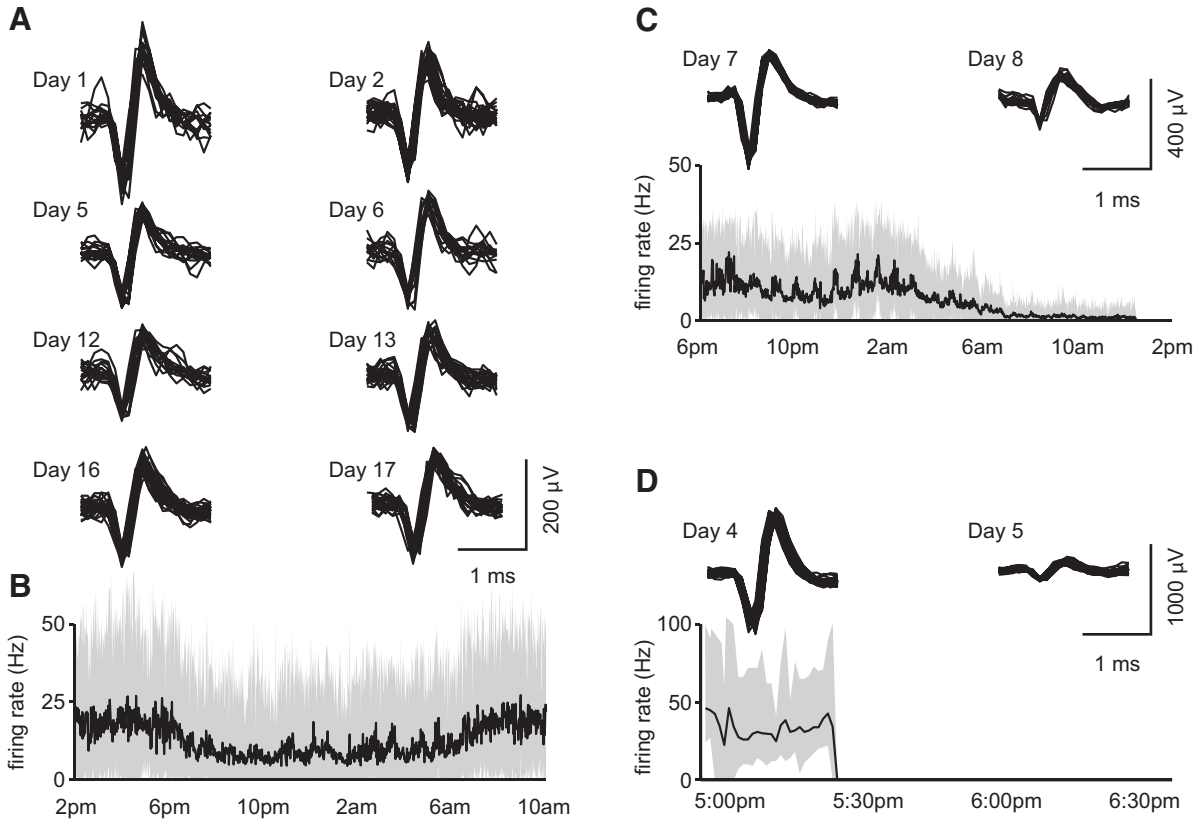

FIG. 4. Stable and unstable recordings obtained during unrestrained behavior using implanted Neurochip circuitry. *A*: sample waveforms for one cell over a 17-day period after positioning the microwire (on day 0). *B*: mean firing rate over consecutive 1-min intervals (dark line) through 18 h of recording for this cell from day 16 to day 17. Also shown in gray are the maximum and minimum firing rates obtained during 100-ms intervals within each minute. Firing rate was lower while the monkey was asleep during the night but was otherwise stable. *C*: recorded firing rate and waveforms for a different cell that showed steadily reduced amplitude between days 7 and 8. Apparent decline in recorded firing rate actually results from failure of the smaller waveforms to satisfy the discriminator parameters. *D*: recorded firing rate and waveforms for a cell exhibiting an abrupt change on day 4.

mum linear correlation coefficient between time-shifted average waveforms (Fig. 6*A*). This similarity score is independent of the absolute amplitudes of waveforms and a value of 1 indicates identically shaped spikes. Waveforms for the same neuron on different days tended to be very similar with 81% of r values >0.95, compared with only 37% of similarity scores calculated between waveforms of different cells (Fig. 6*B*). Although this suggests that in general spike shapes remained consistent, the overlap between the distributions shown in Fig. 6*B* indicates that spikes from different cells could also exhibit similar waveforms. Thus a consistent spike shape alone does not provide conclusive evidence that the same individual neurons are present in recordings on subsequent days.

Postmortem histology

Cresyl-stained slices from monkey Y revealed clear electrode tracks running down the anterior bank of the central sulcus along the edge of the gray/white matter border (Fig. 7*A*). Dense glial scarring surrounded these tracks and electrode tips (Fig. 7*B*). The orientation revealed by this histology helps explain the successful yield and large waveform amplitudes obtained during this experiment because many tracks ran close to layer V where large pyramidal cell bodies are located. For this reason movable microwire arrays may be particularly applicable to recording down the banks of sulci where cells can be found at many different depths.

DISCUSSION

Suitability of movable microwire arrays for long-term recording

In our experience movable microwire arrays provide a favorable combination of high signal-to-noise ratios (SNRs), excellent neuronal stability during free behavior, and long-term performance. Large-amplitude waveforms can be acquired consistently on moving the microwires into fresh tissue (at the time of writing, the implant in monkey K is still recording clean neurons after 22 mo) and the movable wires allow recording from multiple sites down the banks of sulci. Although the yield of simultaneously recorded neurons is relatively low, individual cells remain well isolated and stable for many days at a time (one cell remained consistent for almost 3 wk before the microwire was moved). This technique is therefore well suited to studying the neural correlates of natural, unrestrained behaviors and processes that extend over periods of several days, such as learning. The implant is simple to construct with readily available components and sufficiently small to be used in conjunction with implanted electronic circuitry for wireless recording. For our experiments, the array was enclosed by a large (6-cm-diameter) chamber, which also housed the electronics and battery. In other situations a smaller implant about the size of a conventional recording chamber would be feasible, or multiple arrays could be implanted to record from different cortical areas. These microwires can

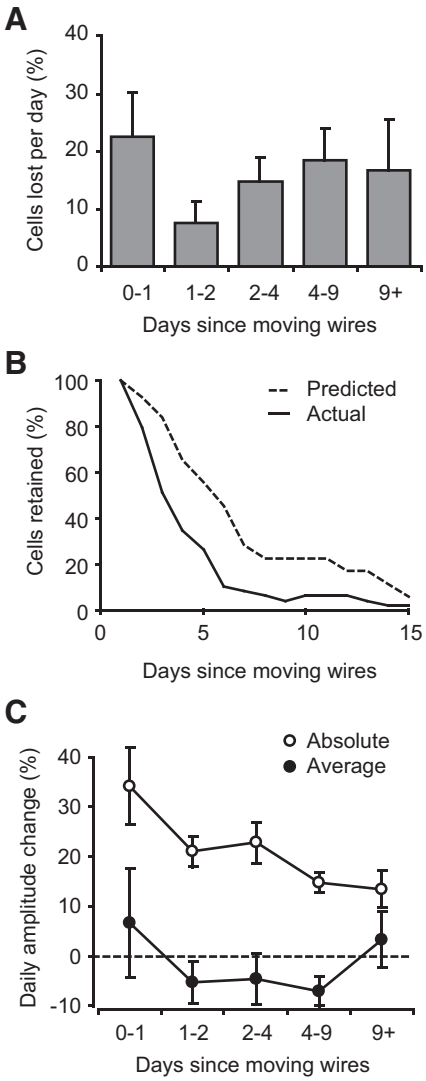

FIG. 5. Analysis of overall cell stability. *A*: mean rate of cell loss per day for different intervals of time following movement of the wires. Bars indicate the SD of loss rate based on the assumption that loss events occur independently with equal probability. *B*: predicted percentage of day 1 cells retained on each subsequent day calculated from mean loss rates (dashed line). Also shown is the actual percentage of day 1 cells that were subsequently recorded (solid line). *C*: mean change in signed (solid circles) and absolute (filled circles) peak-to-peak amplitude per day for different intervals of time following movement of the wires. Error bars indicate SEs.

also be used to deliver intracortical microstimulation (e.g., Jackson et al. 2006a).

Movable microwires may be especially useful for experiments that require repeated monitoring of small populations of cells over periods of several days, for example, to study neural plasticity during learning. In such cases, continued identification of specific cells may be critical to unambiguous interpretation of the data. In our experiments, a range of corroborating evidence supported the general consistency of cell identities through the recordings, including clean ISI histograms, stability of waveforms, and preserved behavioral correlations over several days. However, no single test can provide a conclusive assurance that individual cells on any given day are the same as those recorded previously. Spike amplitudes could vary considerably over a 24-h period and in many learning experiments a change in behavioral tuning may be the observation of interest. Different cells could often have similar waveforms (Fig. 6*B*) such that a consistent spike shape from day to day is no guarantee of identity. In some cases (e.g., pyramidal tract neurons), antidromic identification by stimulating output pathways may be useful in this regard (Lemon 1984), although the stability of antidromic latencies and thresholds over many days remains to be demonstrated. In light of these issues, continuous recording with implanted microprocessors or telemetry systems may prove valuable for future experiments, revealing as it does both gradual and abrupt changes in spike shape.

Comparison with alternative techniques

The range of commercially available chronic electrode and microdrive designs has expanded considerably in recent years, although a review of the relative merits of each is beyond the scope of this article. Here we will contrast several recent reports of long-term recordings from the macaque cortex. Performance of the movable microwire arrays can be compared meaningfully with fixed electrode arrays (Nicolelis et al. 2003; Santhanam et al. 2007; Suner et al. 2005) and miniature microdrives carrying conventional sharp electrodes (Cham et al. 2005; Gray et al. 2006; Wilson et al. 2003). The number of electrodes in high-density implants such as fixed microwires (Nicolelis et al. 2003) or the Utah array (Suner et al. 2005) can yield large cell counts, and these devices may be sufficiently

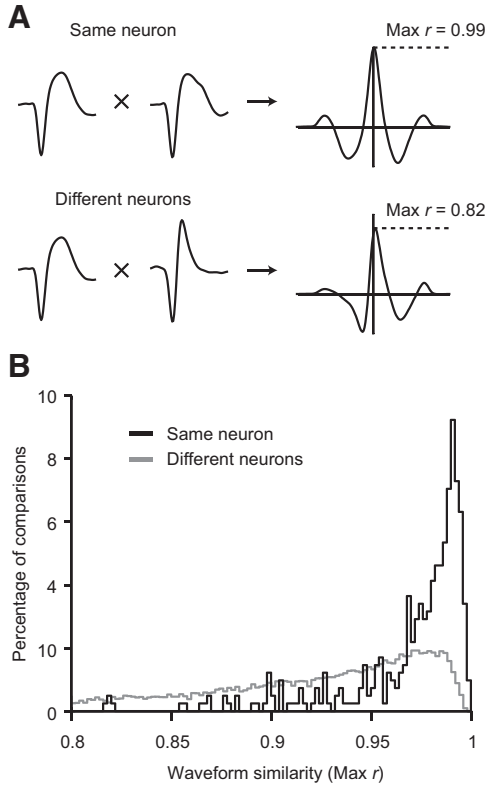

FIG. 6. Similarity between spike shapes for the same neuron on different days vs. different neurons. *A*: spike-shape similarity was quantified by the peak of the normalized cross-correlation function between average waveforms; a value of 1 indicates identical spike shapes, irrespective of absolute spike amplitudes. *B*: histogram of all spike-shape similarities for the same neuron on different days (dark line), and between all pairs of different neurons in the entire data set (gray line).

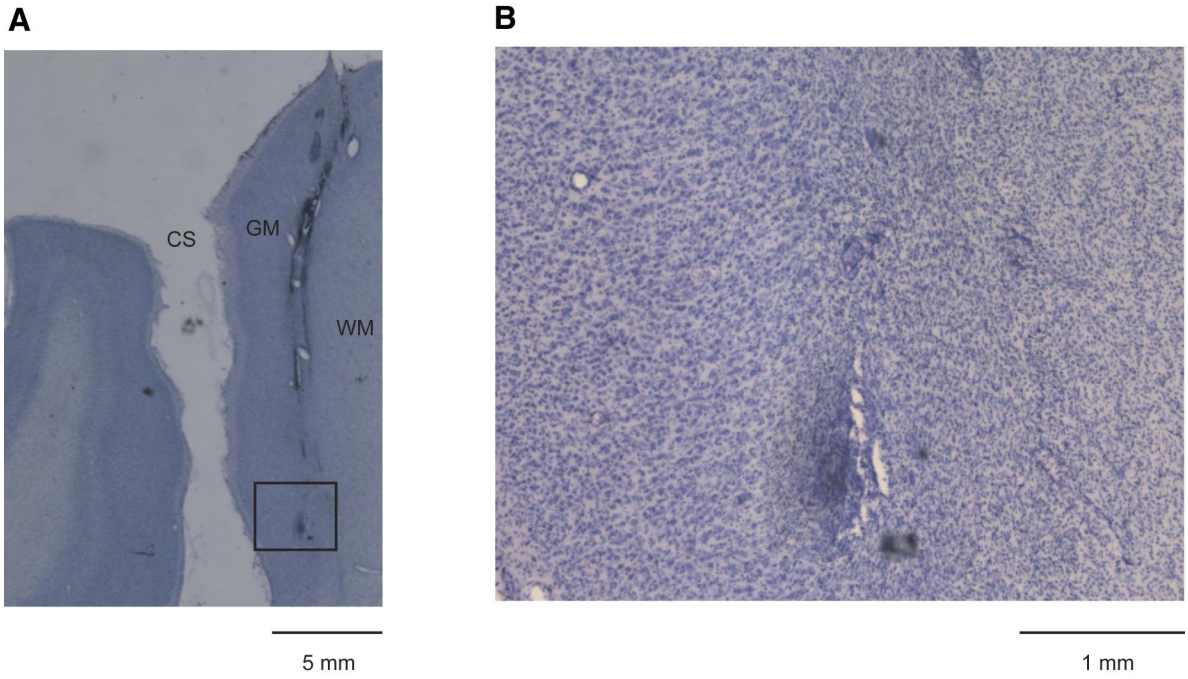

FIG. 7. Postmortem histology from monkey Y. *A*: cresyl-stained coronal sections showing gliosis surrounding electrode tracks running down the anterior bank of the CS along the gray matter (GM) and white matter (WM) border. *B*: increased magnification of the end of one electrode track located close to large layer V pyramidal cells.

small and safe for clinical use as BCIs. Long-term performance continues to improve, with spike recordings reported several years after implantation (Sandler et al. 2005; Suner et al. 2005). Stability of individual cells recorded on the Utah array over periods of several days has recently been demonstrated using an implanted recording system (Santhanam et al. 2007). Amplitude variations of a magnitude similar to that of the present study were reported. However, comparison with published data for both fixed microwires and Utah arrays suggests that the movable microwires yield recordings with substantially higher SNR. Suner et al. (2005) reported a mean SNR value of 4.8 for signals ranked as "high quality" on a Utah array, whereas Nicolelis et al. (2003) reported a mean SNR of 5.5 for fixed microwire recordings. By contrast, the mean SNR value for our movable microwire recordings was 14.5. This improvement is also evident in the mean peak-to-peak amplitude (248 μV) compared with that of fixed microwires (115 μV; Nicolelis et al. 2003). Furthermore, a single well-isolated unit was most often obtained with our method, compared with the multiunit recordings often obtained with fixed arrays. Although it remains to be seen whether single- or multiunit data will be most appropriate for BCI applications (Carmena et al. 2003), isolating individual cells has clear benefits for scientific studies. Even if waveforms are sufficiently distinct to be separated, the presence of multiple cells on a channel may compromise the reliability of identifying neurons over several days, given the changes of amplitude that can occur.

One explanation for the high SNR and prevalence of single units on these electrodes may be the ability to accurately adjust their depth to position the tips within layer V, close to the large pyramidal cells. The ability to repeatedly advance individual electrodes into fresh tissue is also likely to be an important factor. A number of groups are working to reduce the tissue response to chronically implanted electrodes (He et al. 2006; Retterer et al. 2004) and the data reported here may offer incentive by demonstrating that significant future improvements in signal-to-noise performance should be possible.

In many ways the converse of these considerations applies to miniature microdrives fixed to the skull (Cham et al. 2005; Gray et al. 2006; Swadlow et al. 2005; Wilson et al. 2003). Such systems yield well-isolated units with good SNR on initially penetrating the cortex, and can reach deeper structures, including the banks of sulci. However, reports suggest that the long-term stability of individual neurons in primates is limited to several days at most (Gray et al. 2006; Wilson et al. 2003). In an attempt to address this issue, Cham et al. (2005) proposed an automated tracking algorithm for continually adjusting electrode depth to maintain cell isolation, although the practicality of this remains to be proven. Stability could possibly be improved using flexible microwires as in our movable array instead of rigid, sharp electrodes, but this would likely require resection of the dura mater in primates. Commercially available screw drives such as the Neuralynx microdrive (Neuralynx, Bozeman, MT) may prove suitable for positioning microwires in primate cortex if the risk of infection can be managed, perhaps using the combination of antibiotic cream and Silastic described in this report. The use of such screw drives would be advantageous in situations requiring calibrated depth measurement. In practice, however, the precise depth control of a microdrive may not confer sufficient long-term advantage to justify the increased implant size. In our experience, many cells changed size or were lost in the first 24 h after moving the microwires, so efforts to optimize specific waveforms on day 0 were often unrewarded, whereas channels with small waveforms subsequently yielded stable, well-isolated cells a day later.

In conclusion, we have described a compact movable microwire array, constructed from readily available materials,

that offers favorable signal-to-noise characteristics, neuronal stability, and long-term performance. This technique allows individual cells in the cortex of nonhuman primates to be followed for several weeks at a time and opens the possibility of studying neural correlates of long-term processes such as plasticity and motor learning.

ACKNOWLEDGMENTS

We thank S. Perlmutter, J. Mavoori, C. Kirby, C. Moritz, S. Zanos, L. Shupe, and S. Baker for assistance.

GRANTS

This work was supported by National Institutes of Health Grants NS-12542 and RR-00166 and the University of Washington Royalty Research Fund.

REFERENCES

Baker SN, Philbin N, Spinks R, Pinches EM, Wolpert DM, MacManus DG, Pauluis Q, Lemon RN. Multiple single unit recording in the cortex of monkeys using independently moveable microelectrodes. *J Neurosci Methods* 94: 5–17, 1999.

Biran R, Martin DC, Tresco PA. Neuronal cell loss accompanies the brain tissue response to chronically implanted silicon microelectrode arrays. *Exp Neurol* 195: 115–126, 2005.

Carmena JM, Lebedev MA, Crist RE, O'Doherty JE, Santucci DM, Dimitrov DF, Patil PG, Henriquez CS, Nicolelis MA. Learning to control a brain-machine interface for reaching and grasping by primates. *PLoS Biol* 1: e42, 2003.

Cham JG, Branchaud EA, Nenadic Z, Greger B, Andersen RA, Burdick JW. Semi-chronic motorized microdrive and control algorithm for autonomously isolating and maintaining optimal extracellular action potentials. *J Neurophysiol* 93: 570–579, 2005.

Eckhorn R, Thomas U. A new method for the insertion of multiple microprobes into neural and muscular tissue, including fiber electrodes, fine wires, needles and microsensors. *J Neurosci Methods* 49: 175–179, 1993.

Gray CM, Goodell B, Salazar R, Baker J. Semi-chronic recording of neuronal activity in monkey visual cortex using a 60-channel microdrive. *Soc Neurosci Abstr* 148.16, 2006.

Griffith RW, Humphrey DR. Long-term gliosis around chronically implanted platinum electrodes in the Rhesus macaque motor cortex. *Neurosci Lett* 406: 81–86, 2006.

He W, McConnell GC, Bellamkonda RV. Nanoscale laminin coating modulates cortical scarring response around implanted silicon microelectrode arrays. *J Neural Eng* 3: 316–326, 2006.

Jackson A, Mavoori J, Fetz EE. Long-term motor cortex plasticity induced by an electronic implant. *Nature* 444: 56–60, 2006a.

Jackson A, Mavoori J, Fetz EE. Correlations between the same motor cortex cells and arm muscles during a trained task, free behavior, and natural sleep in the macaque monkey. *J Neurophysiol* 97: 360–374, 2007.

Jackson A, Moritz CT, Mavoori J, Lucas TH, Fetz EE. The Neurochip BCI: towards a neural prosthesis for upper limb function. *IEEE Trans Neural Syst Rehab Eng* 14: 187–190, 2006b.

Johnson JL, Welsh JP. Independently moveable multielectrode array to record fast-spiking neurons in the cerebral cortex during cognition. *Methods* 30: 64–78, 2003.

Kralik JD, Dimitrov DF, Krupa DJ, Katz DB, Cohen D, Nicolelis MA. Techniques for chronic, multisite neuronal ensemble recordings in behaving animals. *Methods* 25: 121–150, 2001.

Lemon RN. Methods for neuronal recording in conscious animals. In: *IBRO Handbook Series: Methods in Neurosciences* (4th ed.), edited by Smith AD. London: Wiley, 1984, p. 1–162.

Mavoori J, Jackson A, Diorio C, Fetz EE. An autonomous implantable computer for neural recording and stimulation in unrestrained primates. *J Neurosci Methods* 148: 71–77, 2005.

Nicolelis MAL. Brain-machine interfaces to restore motor function and probe neural circuits. *Nat Rev Neurosci* 4: 417–422, 2003.

Nicolelis MAL, Dimitrov D, Carmena JM, Crist R, Lehew G, Kralik JD, Wise SP. Chronic, multisite, multielectrode recordings in macaque monkeys. *Proc Natl Acad Sci USA* 100: 11041–11046, 2003.

Nordhausen CT, Maynard EM, Normann RA. Single unit recording capabilities of a 100 microelectrode array. *Brain Res* 726: 129–140, 1996.

O'Keefe J, Recce ML. Phase relationship between hippocampal place units and the EEG theta rhythm. *Hippocampus* 3: 317–330, 1993.

Retterer ST, Smith KL, Bjornsson CS, Neeves KB, Spence AJ, Turner JN, Shain W, Isaacson MS. Model neural prostheses with integrated microfluidics: a potential intervention strategy for controlling reactive cell and tissue responses. *IEEE Trans Biomed Eng* 51: 2063–2073, 2004.

Sandler AJ, Dewey KS, Nicolelis MAL. Long-term neuronal recordings from nonhuman primates. *Soc Neurosci Abstr* 402.8, 2005.

Santhanam G, Linderman MD, Gilja V, Afshar A, Ryu SI, Meng TH, Shenoy KV. HermesB: a continuous neural recording system for freely behaving primates. *IEEE Trans Biomed Eng* doi:10.1109/TBME.2007.895753.

Schwartz AB, Cui XT, Weber DJ, Moran DW. Brain-controlled interfaces: movement restoration with neural prosthetics. *Neuron* 52: 205–220, 2006.

Steriade M, Nunez A, Amzica F. A novel slow (<1 Hz) oscillation of neocortical neurons in vivo: depolarizing and hyperpolarizing components. *J Neurosci* 13: 3252–3265, 1993.

Suner S, Fellows MR, Vargas-Irwin C, Nakata GK, Donoghue JP. Reliability of signals from a chronically implanted, silicon-based electrode array in non-human primate primary motor cortex. *IEEE Trans Neural Syst Rehabil Eng* 13: 524–541, 2005.

Swadlow HA, Bereshpolova Y, Bezdudnaya T, Cano M, Stoelzel CR. A multi-channel, implantable microdrive system for use with sharp, ultra-fine "Reitboeck" microelectrodes. *J Neurophysiol* 93: 2959–2965, 2005.

Szarowski DH, Andersen MD, Retterer S, Spence AJ, Isaacson M, Craighead HG, Turner JN, Shain W. Brain responses to micromachined silicon devices. *Brain Res* 983: 23–35, 2003.

Wilson FA, Ma YY, Greenberg PA, Ryou JW, Kim BH. A microelectrode drive for long term recording of neurons in freely moving and chaired monkeys. *J Neurosci Methods* 127: 49–61, 2003.

Wilson MA, McNaughton BL. Dynamics of the hippocampal ensemble code for space. *Science* 261: 1055–1058, 1993.